

Structure of human follicle-stimulating hormone in complex with its receptor

Qing R. Fan¹ & Wayne A. Hendrickson^{1,2}

¹Department of Biochemistry and Molecular Biophysics and, ²Howard Hughes Medical Institute, Columbia University, New York, New York 10032, USA

Follicle-stimulating hormone (FSH) is central to reproduction in mammals. It acts through a G-protein-coupled receptor on the surface of target cells to stimulate testicular and ovarian functions. We present here the 2.9-Å-resolution structure of a partially deglycosylated complex of human FSH bound to the extracellular hormone-binding domain of its receptor (FSHR_{HB}). The hormone is bound in a hand-clasp fashion to an elongated, curved receptor. The buried interface of the complex is large (2,600 Å²) and has a high charge density. Our analysis suggests that all glycoprotein hormones bind to their receptors in this mode and that binding specificity is mediated by key interaction sites involving both the common α - and hormone-specific β -subunits. On binding, FSH undergoes a concerted conformational change that affects protruding loops implicated in receptor activation. The FSH-FSHR_{HB} complexes form dimers in the crystal and at high concentrations in solution. Such dimers may participate in transmembrane signal transduction.

FSH is secreted from the pituitary gland to regulate reproduction in mammals^{1,2}. In females, FSH targets a receptor (FSHR) expressed only on granulosa cells, and induces the maturation of ovarian follicles^{1,3}. The levels of both FSH and FSHR rise until the middle of oestrus, and then fall precipitously as luteinizing hormone (LH) triggers ovulation. In males, FSH stimulates sertoli cell proliferation in testes and supports spermatogenesis^{1,3}. FSH is used clinically to treat anovulatory women and infertile men, and we expect that a molecular understanding of the FSH interaction with FSHR may assist in the design of contraceptive antagonists and alternative agonists.

FSH is a member of the glycoprotein hormone family, which also includes LH, chorionic gonadotropin (CG) and thyroid-stimulating hormone (TSH)⁴. These glycoprotein hormones are disulphide-rich heterodimers consisting of non-covalently associated α - and β -subunits⁴. In a given species, they share a common α -chain but derive functional specificity from different β -chains⁴. Crystal structures of human CG (hCG)^{5,6} and FSH⁷ both reveal elongated molecules with similar folds for the α - and β -chains, and a cysteine-knot motif in the central core of each subunit. The interactions between the glycoprotein hormones and their corresponding receptors are highly selective, with very few cases of cross activity³.

The glycoprotein hormones act through specific G-protein-coupled receptors (GPCRs) on target cell surfaces^{1,8,9}. FSH and TSH bind to FSHR and TSHR, respectively; LH and CG both bind to the same receptor, LHR. These receptors belong to a subfamily of GPCRs called leucine-rich-repeat-containing GPCRs (LGRs), which are characterized by an extracellular domain with multiple leucine-rich repeats (LRRs) and a rhodopsin-like domain of seven transmembrane (7TM) helices¹⁰. Unlike most other GPCR proteins, which have relatively short extracellular segments and bind small molecule ligands, the LGRs have large ectodomains and bind protein ligands including glycoprotein hormones and relaxin¹⁰.

Ligand binding and receptor activation appear to be distinct activities of glycoprotein hormone receptors. The extracellular domains of glycoprotein hormone receptors are responsible for the specificity and high affinity of ligand binding (typically at sub-nanomolar dissociation constant (K_d) values^{2,8}), whereas the transmembrane domains are responsible for receptor activation and signal transduction through G proteins^{1,8,9}. Hormone binding to the ectodomain of a glycoprotein hormone receptor somehow prompts changes in the 7TM domain that propagate across the plasma

membrane to elicit guanine nucleotide exchange in a heterotrimeric G_s protein. Activation of adenylyl cyclase for the production of cAMP ensues, thereby initiating a signalling cascade that leads to steroid synthesis^{1,8,9}. In an effort to understand ligand binding and receptor stimulation in this signalling pathway, we have determined the crystal structure of human FSH bound to the hormone-binding domain of its receptor. Our finding of receptor-mediated dimers in the crystal prompted us to study dimerization in solution and to contemplate its role in signal transduction on the membrane.

Assembly of the FSH-FSHR_{HB} complex

Human FSH and a truncated ectodomain of human FSHR were co-secreted as a stable complex from insect cells using the baculovirus expression system. The α - and β -subunits of the heterodimeric FSH were joined into a single chain with a Gly/Ser-rich linker from the carboxy terminus of the β -subunit to the amino terminus of the α -subunit; similar FSH and CG constructs, but with different linkers, have been shown to retain a wild-type level of function¹¹⁻¹³. All glycoprotein hormone receptors comprise a series of LRRs flanked at each end by cysteine clusters. Refolding experiments of recombinant LHR indicate that the N-terminal cysteine cluster is required for proper folding (data not shown). A truncated FSHR consisting of the N-terminal cysteine cluster and the LRRs forms a stable complex with FSH, indicating that the C-terminal cysteine-rich region of the ectodomain is not required for hormone binding. We therefore define the N-terminal cysteine cluster together with the LRRs as the hormone-binding domain of the receptor (FSHR_{HB}).

Structure determination

Co-secreted FSH and FSHR_{HB} form a 1:1 complex as demonstrated by its retention time upon gel filtration chromatography (data not shown). The fully glycosylated FSH-FSHR_{HB} complex could be crystallized in several different forms, the best of which only diffracted to 9 Å spacings. Partial deglycosylation using a combination of endoglycosidases F2 and F3 yielded a new crystal form, which diffracted to 2.9 Å spacings. The crystals are of space group C2, with two complexes in the asymmetric unit. The complex structure was determined by molecular replacement. The positions of the two hormone molecules were located using the known structure of human FSH⁷ as the search model. Partial phases obtained from the molecular replacement solution were improved by two-fold molecular averaging to yield electron density for the

bound receptor. A complete model of the complex was developed iteratively and refined ultimately at 2.9 Å resolution to an *R*-value of 21.9% (*R*_{free} = 25.9%).

Receptor structure consisting of irregular repeats

FSHR_{HB} is formed from its LRR winding into the shape of a slightly curved tube (Fig. 1a, b; see also Supplementary Fig. S1). As predicted from sequence considerations¹⁴ and as found in other LRR structures¹⁵, its concave inner surface is an untwisted, non-inclined β-sheet and its tubular hydrophobic core is filled by LRR namesake leucines and other large hydrophobic residues. The repeats themselves are highly irregular in length and conformation, and particularly so in the outer surface returns. Regular structure in the convex outer surface is limited to seven short β-strands in three sheets (Fig. 1c). Unexpectedly, the N-terminal flanking sequence (residues 18–46) contains the first of the LRR repeats. This segment is further integrated into the structure by an antiparallel β-strand added before the inner β-sheet and by two disulphide bridges (Cys 18–Cys 25 and Cys 23–Cys 32) (Fig. 1a; see also Supplementary Fig. S2).

Unlike other known LRR structures, the curvature of FSHR_{HB} is steeply graded; the C-terminal portion (repeats 7–10) has the signature horseshoe-like curvature of LRR proteins whereas the N-terminal portion of the inner β-sheet (repeats 1–7) is nearly flat. Apart from repeat 1, the overall fold of FSHR_{HB} is likely to be conserved in LHR and TSHR, and across mammalian species, because Leu/Ile/Phe residues in the hydrophobic core of FSHR_{HB} are conserved at equivalent positions in the sequences from LHR and TSHR (Fig. 2c) and almost all repeat irregularities are also conserved. We are describing FSHR_{HB} structural details and comparisons to other LRR proteins elsewhere.

A hand-clasp binding mode

The structure of the FSH–FSHR_{HB} complex shows FSH bound into the concave face of the curved receptor domain in a manner that resembles a hand clasp (Figs 1a, b and 2a), roughly as in our prediction¹⁴. The long axis of FSH is perpendicular to the FSHR_{HB} tube and aligned with receptor β-strands. All ten parallel β-strands and the loops just C-terminal to the β-sheet are in contact with FSH (Fig. 3a; see also Supplementary Fig. S1). The receptor wraps around the middle section of the hormone molecule, interacting with C-terminal segments of both FSH-α and FSH-β as well as the αL2 and βL2 loops. The hormone orientation is such that loops βL1 and βL3 extend out from the C-terminal tips of the receptor

inner sheet, whereas loops αL1 and αL3 protrude away from the base.

The footprints of hormone and receptor onto their partner surfaces (Fig. 2a; see also Supplementary Fig. S1) demonstrate the substantial involvement of both FSH subunits in the interaction with FSHR_{HB}. A total of 2,600 Å² of solvent-accessible surface area from the isolated components is buried into the interface between FSH and FSHR_{HB}. Most of this interface involves the packing of two rather flat surfaces: one formed by the seven N-terminal parallel β-strands of FSHR_{HB} is matched with one from the C-terminal segment of FSH-α and the C-terminal ‘seat-belt’ segment of FSH-β. The rest comes from the αL2 loop with its helical segment clamping over the edge of FSHR_{HB} at the β-strand tips of LRRs 2–6, and from the βL2 loop fitting against the curved C-terminal repeats 8–10. A significant consequence of this geometry is that a swathe of the most deeply buried interfacial receptor residues (Fig. 2c; see also Supplementary Fig. S3) lies across the C-terminal end of the parallel β-sheet (Fig. 3a). Half of these FSHR_{HB} residues (L55, N79, K104, N129, Q152, D153 and K179) are buried by contacts with both FSH-α and FSH-β (Fig. 2a, magenta).

The interface between hormone and receptor is bare of carbohydrate groups. Sufficient density was found to model carbohydrate residues (1–3) at all four potential glycosylation sites on the hormone (FSH-α N52 and N78; FSH-β N7 and N24) and at the one verified glycosylation site on our receptor construct (N191)¹⁶. All of these sites are remote from the interface (Fig. 1a, b). Even the closest carbohydrate moiety, at FSH-α N52, faces away from the receptor interface. Glycosylation at FSH-α N52 has been implicated in signalling but not in binding². Natural mutations located at or close to the conserved glycosylation site of FSHR (N191I, A189V) have been shown to cause inactivation of the receptor², possibly by affecting the proper folding of FSHR¹⁶.

Charge complementarity in a universal binding interface

Several lines of evidence suggest that the mode of binding seen here between FSH and FSHR_{HB} probably also pertains to other mammalian glycoprotein hormones and their receptors. First, highly similar structures for human FSH⁷ and CG^{5,6}, and highly conserved sequences for LH and TSH, including identical α-chains within a species, point to a common ligand structure in the complex. Second, for reasons noted above, we expect the structure of the hormone-binding domain to be essentially the same in all glycoprotein hormone receptors. Third, previous studies on the different systems^{1,8,9} implicate the very structural elements found in our FSH–

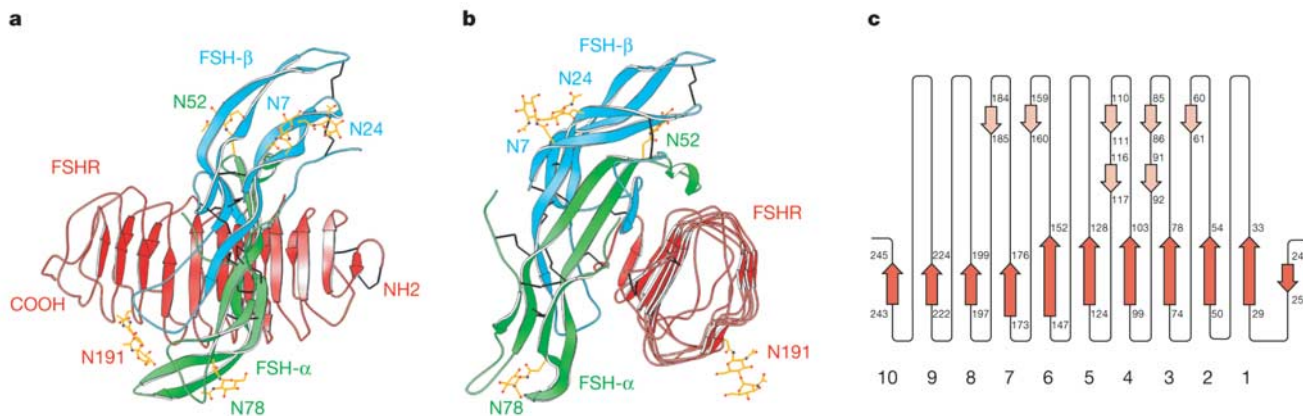


Figure 1 Crystal structure of human FSH bound to FSHR_{HB}. **a, b**, Ribbon diagram of the complex structure shown in two views related by a 90° rotation about the vertical axis. FSH α-chains and β-chains are in green and cyan, respectively. FSHR_{HB} is in red. The observed N-linked carbohydrates at N52 and N78 of FSH-α, N7 and N24 of FSH-β, and

N191 of FSHR_{HB} are in yellow. Disulphide bonds are in black. **c**, Schematic diagram of the topology of FSHR_{HB} structure. β-Strands are shown as arrows. Red represents strands located at the concave face of FSHR_{HB}; pink represents strands on the convex face.

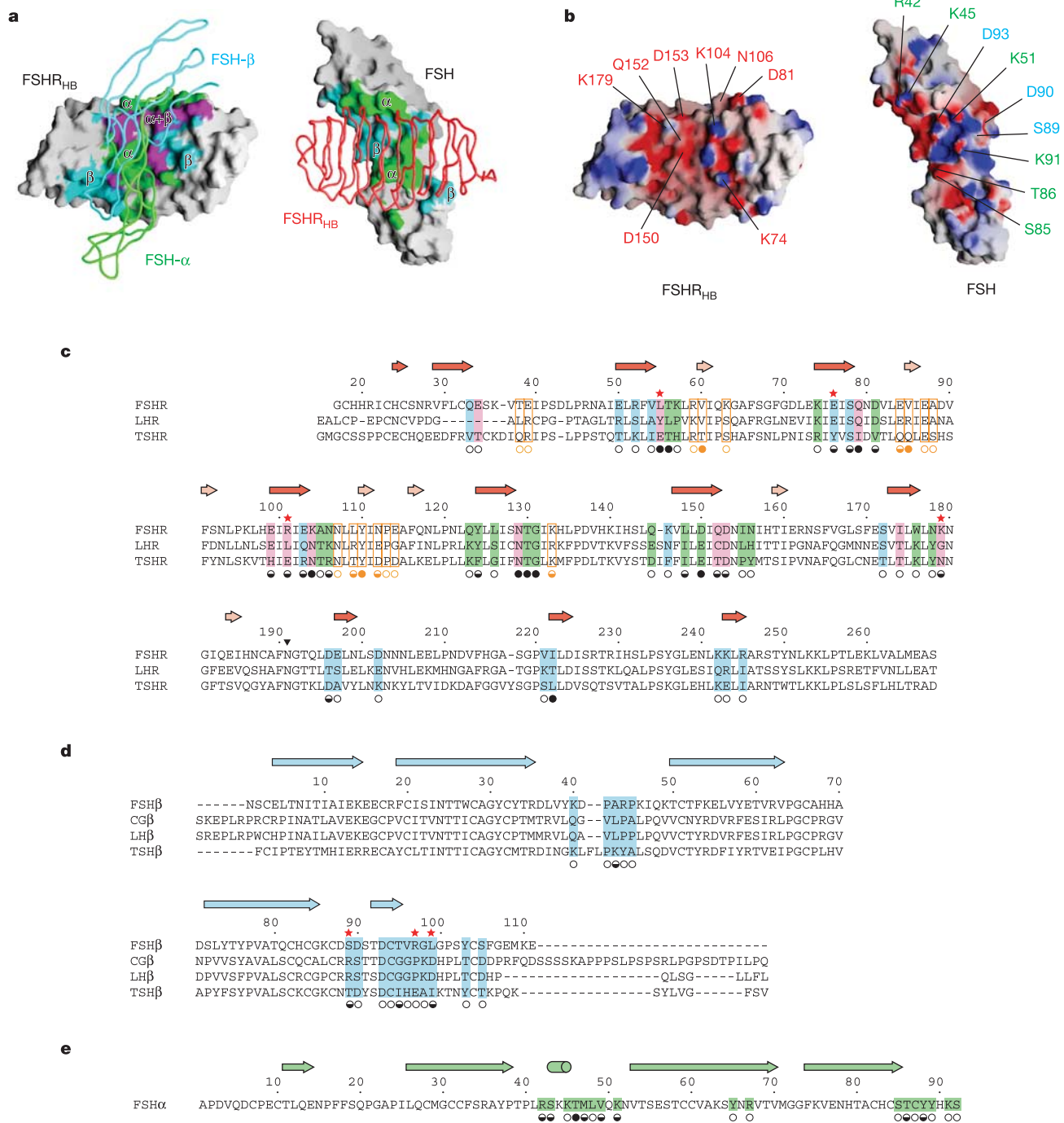


Figure 2 Recognition of FSH by FSHR_{HB}. **a**, The left panel shows the molecular surface of FSHR_{HB} with the imprint of bound FSH (C α trace in green for α - and cyan for β -chains). Coloured patches represent FSHR_{HB} residues that are buried at the receptor–hormone interface by FSH- α alone (green), by FSH- β alone (cyan), or both FSH- α and FSH- β (magenta). The right panel shows the molecular surface of FSH with the imprint of FSHR_{HB} (C α trace in red). Green denotes residues of FSH- α buried by FSHR_{HB}; cyan represents buried FSH- β residues; magenta represents buried FSH- α and FSH- β residues. **b**, Electrostatic potential surface of FSHR_{HB} (left) and FSH (right). Residues of FSHR_{HB} are marked red; residues of the FSH- α and FSH- β chains are in green and cyan, respectively. **c–e**, Sequence alignment. Secondary structure assignments are shown as arrows for β -strands and cylinders for α -helices. For each residue buried at the receptor–ligand interface or the receptor dimer interface, the fractional solvent accessibility is indicated by an open circle if it is greater than 0.4, a half-

filled circle if it is 0.1–0.4, and a filled circle if it is less than 0.1. Residues implicated in binding specificity are marked by asterisks. **c**, Human FSHR, LHR and TSHR sequences in the region of the hormone-binding domain. β -Strands located at the concave face of FSHR are coloured red, whereas strands on the convex face are in pink. FSHR_{HB} residues buried at the receptor–ligand interface by FSH- α alone (green), FSH- β alone (cyan), or both FSH- α and FSH- β (magenta) are highlighted. FSHR_{HB} residues buried at the receptor dimer interface are boxed in orange. N-linked glycosylation is marked by a black triangle. **d**, Human FSH, CG, LH and TSH β -chain sequences. FSH- β residues buried at the receptor–ligand interface are highlighted in cyan. **e**, The common human α -chain sequence. FSH- α residues buried at the receptor–ligand interface are highlighted in green.

FSHR_{HB} complex to be involved in the interaction: namely the LRRs of the receptor and the C-terminal segments of the hormone subunits. Last, residues in the receptor homologues at positions where FSHR_{HB} contacts FSH- α are consistent with a common mode of binding (Fig. 2c). Many of these residues are conserved, and several are charged groups interacting with complementary groups on the hormone.

The interface between FSH and FSHR_{HB} has an exceptionally high buried-charge density in comparison to other protein complexes (1.13 charges per nm²; Q.F. & W.A.H., unpublished data). The electrostatic potential surfaces of the hormone and receptor in the interface are predominately positive and negative, respectively, although less uniformly than in the putative CG-LHR complex¹⁴. The electropositive and electronegative patches in the interface reflect direct interactions between residues with complementary charges (Fig. 2b), many of which are conserved in the homologues. Two invariant acidic residues (D150 and D153 in FSHR) make salt bridges with basic residues from FSH- α (K91 and K51). In addition, D81 from FSHR_{HB} (also Asp in LHR) forms charge-mediated interactions with R42 and K45 of the α L2 loop of FSH. These findings are consistent with previous studies. Charge reversal mutagenesis of E132 and D135 individually to Lys in LHR (residues corresponding to D150 and D153 in FSHR) abolished hCG binding¹⁷; mutation of FSH- α residues K51 (ref. 18) or K91 (ref. 19) to Ala caused the loss of receptor-binding activity; and inhibition of hormone binding using synthetic peptides indicated that the α L2 regions of both human CG and TSH are involved in receptor binding^{20,21}.

Specificity jointly mediated by hormone α - and β -subunits

Having common α -chains within a species, glycoprotein hormones

must be distinguished by their β -chains. Important discriminating determinants of receptor binding have been localized to β -chain C-terminal segments^{22–25} that correspond to a unique seat-belt feature of the hormone structures^{5–7}. The C-terminal end of the β -subunit embraces the α -subunit and fastens into place via a disulphide tether back to the body of the β -subunit^{5–7}. The seat-belt segment of FSH- β (89–105, Fig. 2d) is indeed at the interface, but it is sandwiched between the α L2 loop and C-terminal segment of FSH- α (Fig. 3a; see also Supplementary Fig. S4). Specificity pockets for residues of FSHR_{HB} form through coordination between discriminating β -chain seat-belt residues and common α -chain residues. The only other part of FSH- β at the interface is the tip of loop β L2 (40–45).

We have analysed interfacial contacts for potential determinants of specificity (Supplementary Table S1 and Fig. S5). Five substantially buried (<40% exposed) FSHR_{HB} residues (L55, E76, R101, K179 and I222; Fig. 2c) both vary among human receptors and make contact with FSH residues that vary among the counterpart hormones. Sequence variations indicate that hormone seat-belt interactions with receptor residues at positions 55 and 179 determine the specificity between FSH and TSH versus LH/CG, whereas residues at positions 76 and 101 distinguish between FSH and TSH. The interaction between position I222 and β L2 does not appear to be strongly discriminating. Other variable residues that are substantially buried in FSHR_{HB} (Q79, E103, K104, Q152 and D196; Fig. 2c) are covered in part by FSH- β but are not in direct contact with it; however, they could be selective in homologous complexes. Although collective interfaces must contribute to specificity, three sites appear to predominate. These focus on receptor residues corresponding to L55, K179 and the combination of E76 and R101 in FSHR.

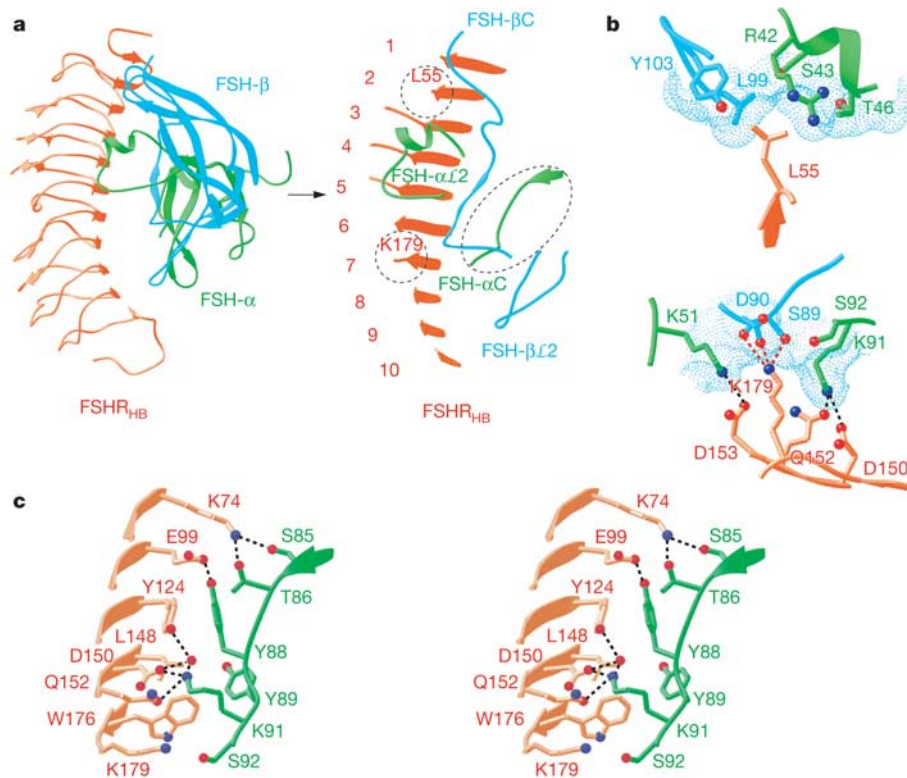


Figure 3 Interactions at the receptor–ligand interface. **a**, Ribbon diagram showing the top view of the FSH–FSHR_{HB} complex. The view in the right panel is tilted to highlight the regions of FSHR_{HB} (red), and FSH- α (green) and FSH- β (cyan) chains that are involved in direct contacts at the receptor–ligand interface. Dashed circles mark the locations of L55

and K179 in the FSHR_{HB} structure. **b**, Detailed views of the interactions at the specificity pockets for L55 and K179 of FSHR_{HB}. The dotted molecular surface of FSH is shown in cyan in each panel. **c**, Close-up stereo view of the interactions between the C-terminal region of FSH- α and FSHR_{HB}.

The molecular surface of FSH provides a shallow pocket for the side chain of L55, which forms hydrophobic interactions with L99 and Y103 of FSH- β and with the aliphatic part of R42 from FSH- α (Fig. 3b). Substitution of L55 in FSHR with the Tyr residue found in LHR resulted in marked loss of function and hormone binding for the mutant receptor²⁶, and it is clear from the structure that steric hindrance would preclude accommodation of the larger Tyr residue in the shallow pocket for L55. The residues in LH or CG (D105 and T109) that correspond to L99 and Y103 in FSH- β are smaller and could potentially form polar interactions or hydrogen bonds with the Tyr residue found in LHR. Conversely, these polar groups in LH/CG would not be complementary to the hydrophobic L55 of FSHR, and indeed FSH binding to FSHR is impaired when residues 95–100 of FSH- β (TVRGLG) are replaced with residues 101–106 of LH- β (GGPKDH)²⁴.

A channel on the molecular surface of FSH hosts the side chain of FSHR K179 (Fig. 3b). The sides of this channel come from K51 and K91 of FSH- α , which make the universal salt bridges discussed above, and its top is capped by S89 and D90 of FSH- β , which form three hydrogen bonds with K179 of FSHR. S89 is substituted with R95 in the β -subunits of CG/LH (Fig. 2d). Adverse interactions of this Arg residue with K179 would be expected to destabilize a potential complex between CG/LH and FSHR. Thus, the structure affords an explanation for extensive mutagenesis studies showing that K179 of FSHR functions as a negative determinant to prevent the binding of CG/LH to FSHR^{26,27}; for example, mutation of K179 to the Gly residue found in LHR gave the mutant FSHR a gain of sensitivity towards hCG²⁶. Moreover, FSH acquires LHR binding activity when residues 88–91 of FSH- β (DSDS) are replaced with their LH- β counterparts (94–97; RRST)²⁴.

A common feature of the specificity pockets for L55 and K179 is the involvement of residues from both the α - and β -chains of FSH, combining stereochemical orientation with specific interactions to mediate selectivity. The third site of selectivity involves the α -chain less directly. Structurally adjacent FSHR_{HB} residues E76 and R101 (Supplementary Fig. S5) interact primarily with R97 and V96 (respectively) from FSH- β , although FSH- α segments contribute to solvent exclusion. Charged side chains do not make hydrogen-bonding contacts here, but repulsion expected from FSHR residues E76 and R101 interacting with the TSH- β Glu and His counterparts of R97 and V96 might explain FSH versus TSH selectivity. Although TSH chimaeras substituted with the FSH- β seat-belt segments failed

to elicit follitropic activity, their reduced thyrotropic responses are compatible with our predictions²⁵. The lengthened β L2 loop of TSH may also participate in selectivity.

Receptor-induced conformational changes in hormone

Although the free and receptor-bound structures of FSH are generally similar, the hormone conformation is substantially changed and appreciably rigidified in the complex (Fig. 4). Free FSH is evidently quite flexible ($C\alpha$ root-mean-squared deviation (r.m.s.d.) of 1.85 Å between copies⁷), and this is especially true at termini and for the α L1, α L3 and β L2 loops at one end. The C terminus of FSH- α and these basal loops are the elements subject to receptor-induced conformational changes, which move them into a fixed conformation ($C\alpha$ r.m.s.d. of 0.71 Å between copies) distinct from any in the free state ($C\alpha$ r.m.s.d. of 1.5–2.9 Å overall; 2.6–6.3 Å for the C terminus of FSH- α and the loops α 13–26, α 66–78, α 88–92 and β 36–47). The conformation of free CG^{5,6} is also distinct from bound FSH.

The most marked change occurs at the C terminus of FSH- α where the terminal segment (88–92) is rotated almost 180° to place its end more than 20 Å away from the free-state position. This segment is buried into the receptor interface where it is fully ordered, whereas the last two residues are disordered in free FSH⁷, as are the last three in hCG^{5,6}. Extensive interactions with the receptor include five direct hydrogen bonds, water-mediated contacts, and hydrophobic interactions (Fig. 3c). Many of these contacts involve residues that are conserved among glycoprotein hormone receptors, consistent with a universal mode of binding.

A key feature of involvement of the FSH- α C terminus in the interface is an aromatic ring-stacking interaction between Y88 of FSH- α (Y127 in human LHR and F130 in TSHR) and Y124 of the receptor. Y88 also forms a hydrogen bond with E99 of FSHR. Altogether, 106 Å² of solvent-accessible surface area from Y88 on FSH- α is buried into the interface. Y88 is the first residue to diverge significantly from the free-state conformation, and its importance in the receptor interaction is demonstrated by experiments where deletion of the terminal residues 88–92 of hCG- α essentially eliminates receptor binding, whereas deletion of just the last four (89–92) retains binding albeit with reduced potency²⁸. Alanine mutagenesis at the C terminus of FSH- α showed that six contiguous residues including Y88 contribute to the FSH–FSHR interaction¹⁹.

The basal loops are locked into their receptor-bound state,

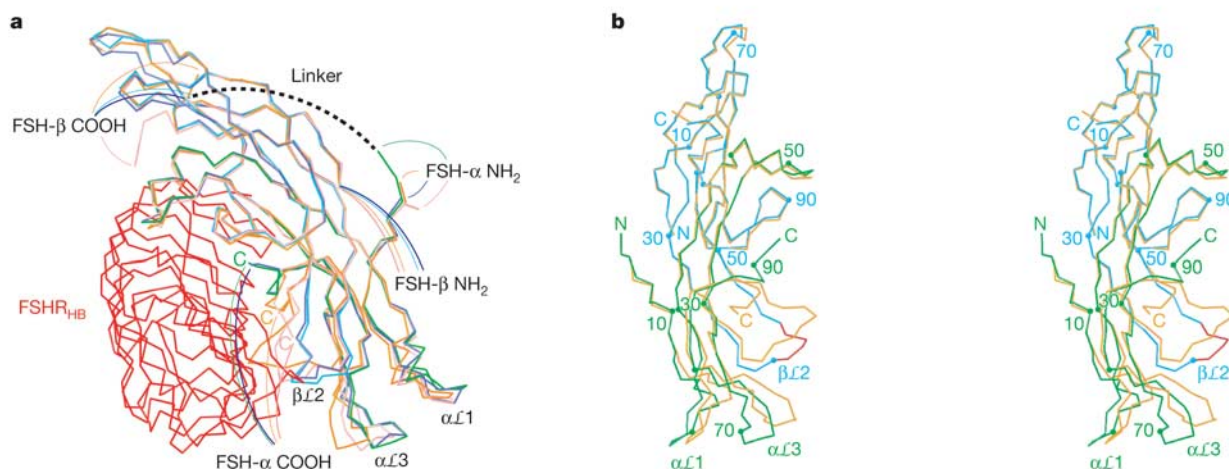


Figure 4 Different conformations in free and receptor-bound FSH. **a**, $C\alpha$ trace superposition of four independent copies of FSH. One protomer of FSH is bound to the FSHR_{HB} shown in red; its α -chain is in green and β -chain in cyan. The second copy of receptor-bound FSH is in blue. The two protomers of free FSH are in orange and pink.

b, Stereo diagram of the superposition of one receptor-bound FSH (α -chain in green; β -chain cyan) with one free hormone (orange). The view is rotated 90° about the vertical axis from **a**. Every 20th residue of the receptor-bound FSH is marked. Red highlights the segment of the β L2 loop that is involved in receptor binding.

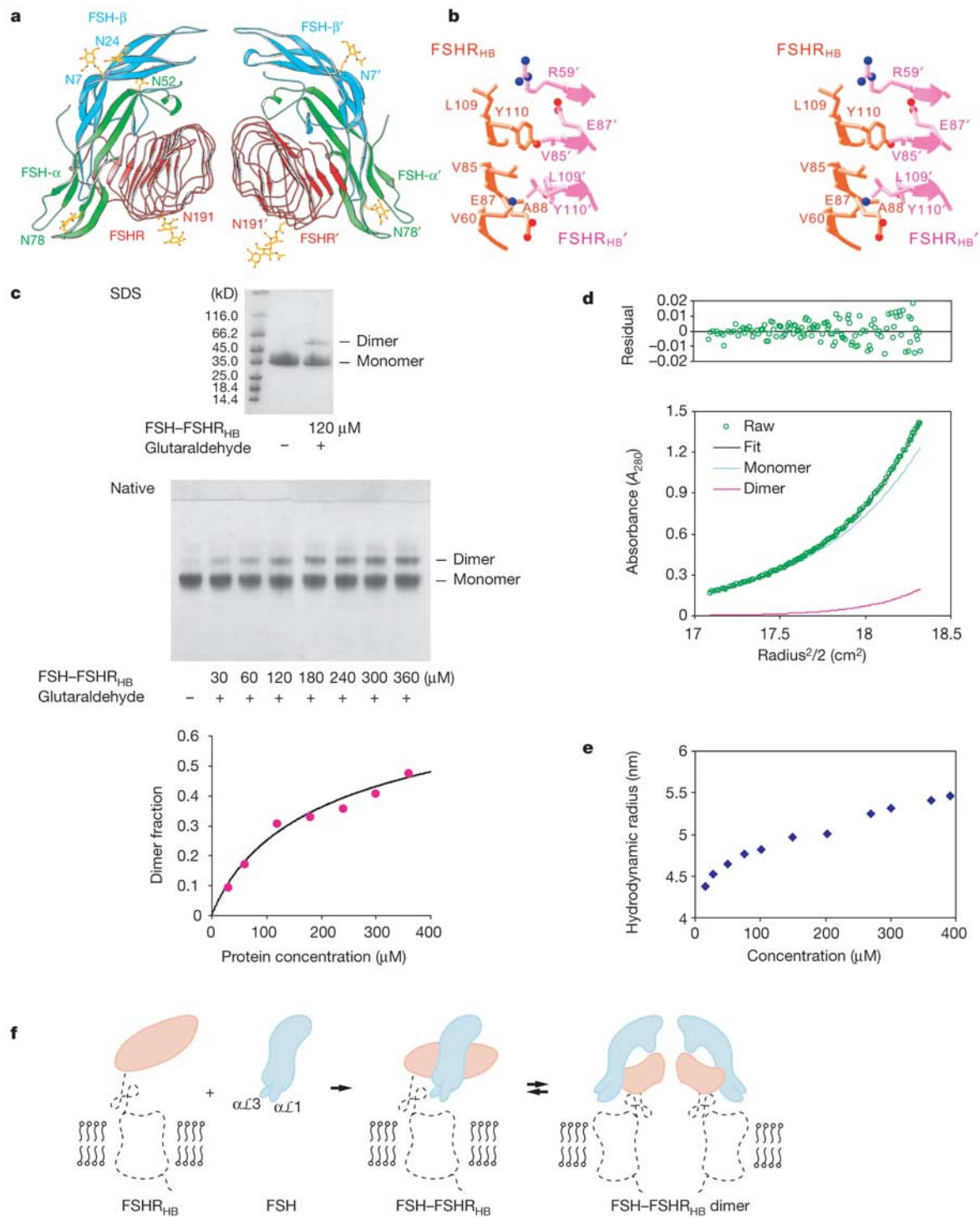


Figure 5 Dimer of the FSH–FSHR_{HB} complex. **a**, Ribbon diagram of a non-crystallographic dimer of the FSH–FSHR_{HB} complex (FSH–FSHR_{HB} and FSH'–FSHR'_{HB}). The receptor is in red, and the α - and β -chains of the hormone are in green and cyan, respectively. **b**, Stereo view of the direct contacts (distances $< 4 \text{ \AA}$) observed at the dimer interface. **c**, Crosslinking of the FSH–FSHR_{HB} complex by glutaraldehyde. The SDS gel contains the FSH–FSHR_{HB} control (lane 2) and 120 μM FSH–FSHR_{HB} complex reacted with 120 μM glutaraldehyde (lane 3). The native gel contains the FSH–FSHR_{HB} control (lane 1), and FSH–FSHR_{HB} complex reacted with glutaraldehyde at a 1:1 molar ratio and at concentrations of 30, 60, 120, 180, 240, 300 and 360 μM (lanes 2–8, respectively). Densities from the dimer bands on native gels as a function of protein concentration were fitted to the dimerization equation with a single K_d ($453 \pm 140 \mu\text{M}$) for six experiments, with two repeated trials for each molar ratio of FSH–FSHR_{HB} to glutaraldehyde (3:1, 3:2, 1:1). The average dimer fraction at each protein concentration is plotted together with the

fitted curve. **d**, Analytical ultracentrifugation analysis of dimer formation by the FSH–FSHR_{HB} complex. Shown are equilibrium sedimentation data (green open circle) taken at 12,000 r.p.m. with a loading concentration of 1.05 mg ml^{-1} , and the best-fit curve (black solid line through the data) for a monomer–dimer reversible equilibrium model. Under the fit, the theoretical sum is deconvoluted into contributions from the monomer (blue line) and dimer (red line) species, respectively. Residuals in absorbance units at 280 nm are shown at the top of the plot. **e**, Apparent hydrodynamic radii of FSH–FSHR_{HB} measured by dynamic light scattering at concentrations of 15, 27, 50, 75, 100, 150, 200, 270, 300, 360 and 390 μM . **f**, Model for FSHR activation by FSH. Projections of the FSH–FSHR_{HB} complex and bovine rhodopsin structures are used to represent the hormone (cyan), the hormone-binding domain (orange) and the linker and transmembrane domain (black dotted trace) of the receptor. The $\alpha\text{L}1$ and $\alpha\text{L}3$ loops of FSH are proposed to contact the transmembrane domain directly.

presumably one favourable for GPCR activation, through interactions that begin with FSH $\beta\mathcal{L}2$ contacts in the complex. Multiple free-state conformations of $\beta\mathcal{L}2$ would conflict with the receptor in the complex and with the receptor-bound conformation of the FSH- α C terminus. Instead, $\beta\mathcal{L}2$ adopts a new and fixed conformation by interacting positively with the three C-terminal LRRs of FSHR_{HB} (Supplementary Table S1 and Fig. S4). Then, it seems that contacts of $\beta\mathcal{L}2$ with its $\alpha\mathcal{L}3$ neighbour move that loop elastically by up to 7.0 Å. In turn, contacts of $\alpha\mathcal{L}3$ with $\alpha\mathcal{L}1$ press the elastic deformation into $\alpha\mathcal{L}1$ to define the final bound-state conformation.

Dimerization of the FSH–FSHR_{HB} complex

The two independent complexes of FSH–FSHR_{HB} in the crystal interact to constitute a dimer. A quasi-two-fold axis of rotational symmetry (rotation $\chi = 175.2^\circ$, screw translation $t_\chi = -1.2$ Å) relates the two protomers, passing between receptor molecules approximately perpendicular to the tube axes, such that the tips of $\alpha\mathcal{L}1$ and $\alpha\mathcal{L}3$ from the hormone are coplanar (Fig. 5a). The dimer interface involves the three-stranded β -sheet (LRRs 2–4) on the outer surface of FSHR_{HB} (Fig. 5b). Y110 (Fig. 2c) contributes prominently in a largely hydrophobic interaction, mediating 21 out of 24 direct carbon–carbon contacts. Because Y110 is completely conserved (Fig. 2c), the homologous receptors may form dimers in a similar manner. The solvent-accessible surface area buried at the dimeric interface is relatively small (940 Å² total from both non-hydrated protomers), which suggests a weak association.

Dimers of the FSH–FSHR_{HB} complex were detected in solution by chemical crosslinking, analytical centrifugation and light scattering. Crosslinking of FSH–FSHR_{HB} with equal or less than equal molar ratios of glutaraldehyde produced dimer bands on SDS and native gels in a concentration-dependent manner. Quantification of dimer formation as a function of protein concentration could be fitted with a K_d of 453 ± 140 μ M (Fig. 5c). Sedimentation equilibrium experiments indicated that the FSH–FSHR_{HB} complex exists in a monomer–dimer equilibrium (Fig. 5d) with a K_d of 388 ± 120 μ M. Dynamic light-scattering measurements for FSH–FSHR_{HB} showed that the apparent hydrodynamic radius increased 25% over the concentration range of 15–390 μ M (Fig. 5e), well beyond the concentration dependence found for non-associating proteins.

Implications for receptor activation

We expect the picture of ligand binding provided by the FSH–FSHR_{HB} complex to apply to all glycoprotein hormone systems, as discussed above. Moreover, glycoprotein hormone receptors have 7TM portions that are very similar, both to one another (~70% sequence identity) and to other rhodopsin-family GPCRs, and when activated they can directly stimulate the same G_s protein used by other GPCRs. Thus, we anticipate a mechanism for receptor activation that is essentially the same for FSHR, LHR and TSHR, and one that has elements in common with other GPCRs²⁹. Now that we have structures in hand for an ectodomain complex with an activating ligand and for rhodopsin³⁰ as an inactive-state model of the 7TM domain, we are in a position to contemplate receptor activation in this system. To do this, we must first understand how the FSH–FSHR_{HB} complex is oriented relative to the 7TM portion. Mapping experiments show that hormone epitopes on both the α -tip ($\alpha\mathcal{L}1$, $\alpha\mathcal{L}3$) and β -tip ($\beta\mathcal{L}1$, $\beta\mathcal{L}3$) are antibody accessible in hCG–porcine LHR (pLHR) ectodomain complexes but accessibility to the α -tip is occluded in complexes with full-length pLHR³¹. Thus, we believe that the complex is oriented as in Figs 1, 4 and 5 relative to a cell surface below it: that is, with α -tips membrane-proximal and the receptor dyad approximately normal to the surface.

At least three models have been suggested for the activation of glycoprotein hormone receptors⁸. One invokes hormone-induced

conformational changes in the ectodomain that directly activate the 7TM domain³²; a second features ectodomain constraints on activity that are released by hormone binding or by certain mutations³³; and a third proposes that it is the hormone when bound to the ectodomain that directly activates the 7TM domain^{14,31,32}. Elements of each might be involved. Although aspects of hormone binding and receptor activation are separable, these models imply a necessary thermodynamic linkage.

We do not yet know the structure of free FSHR_{HB}, but based on other LRR structures¹⁵ it seems unlikely that any substantial changes in this domain accompany hormone binding (model 1). Certainly nothing of the kind found in the dimeric ectodomains of metabotropic glutamate receptors³⁴ is feasible here. Moreover, the finding that LHR/FSHR chimaeras with swapped extracellular domains respond fully in accord with hormone-binding selectivity³² implies that membrane-proximal surfaces of the hormone-binding domain, which are quite variable, are not involved in activation.

The model of hormone-released inhibition (model 2) derives from observations of ectodomain mutations that confer hormone-independent, constitutive activity to the receptor³³. These mutations, at receptor counterparts of S273 just beyond the end of FSHR_{HB}, are in a conserved segment in the linker connecting the LRRs to the 7TM domain. Apart from conservation at each end and at six cysteine positions, which are thought to create a condensed structure by disulphide bridging, these linkers are highly variable among receptors in sequence and length (87–137 residues). Whether S273 mutations truly release inhibition or activate positively is unclear because receptors lacking ectodomains are inactive⁸ or not fully active³³. Semantics aside, involvement of the linker region in activation is apparent both from these mutations and from the requirement for tyrosine sulphation at a site towards the membrane end of the linker³⁵. The $\alpha\mathcal{L}1/\alpha\mathcal{L}3$ tips in the complex protrude towards a space where they might interact with the linker structure in normal, hormone-directed signalling.

The FSH–FSHR_{HB} structure is fully compatible with direct interactions between the α -tips of the hormone in its receptor-bound conformation and the 7TM domain and linker elements (model 3). The $\beta\mathcal{L}2$ loop would seem to be hidden from direct contact, but its integrity would be essential to generate the bound conformation of $\alpha\mathcal{L}1$ and $\alpha\mathcal{L}3$ (Fig. 4). Such activation might be mediated either by contacts with 7TM loops or, plausibly, by insinuation into the 7TM barrel after displacement of the second extracellular loop (EL2)³⁰. Several experiments are consistent with this model, including the chimaeric exchanges³², antibody occlusion³¹, EL2-peptide inhibition of signalling and α -tip antibody access³¹, and signal-enhancing $\alpha\mathcal{L}1$ mutations³⁶. Moreover, the remoteness of the carbohydrate at FSH- α N52 from conceivable activation sites is consistent with results from disulphide-stabilized hCG showing no effect on activity as a result of mutational deglycosylation at this site³⁷. On the other hand, the structure is incompatible with experiments implicating the C terminus of the α -subunit in receptor activation³⁸.

Our observation of dimerization by the FSH–FSHR_{HB} complex suggests that such dimerization may also have a role in glycoprotein hormone receptor function (Fig. 5f). Indeed, dimerization is increasingly found to be important for signal transduction by GPCRs³⁹. Although the dimeric interaction seen for soluble FSH–FSHR_{HB} is quite weak ($K_d \sim 400$ μ M), this affinity is expected to be enhanced substantially when the receptors are anchored in the membrane⁴⁰. Dimerization of hormone–receptor complexes is consistent with the co-expression of mutant receptor defective in hormone binding with others defective in signal transduction, whereby ligand-induced cAMP production is reconstituted^{41,42}, and also with direct measures of self-association through co-immunoprecipitation of differentially tagged receptors⁴³ or by fluorescence-resonance energy transfer experiments⁴⁴. Puzzles do remain, however, as receptor C termini in the dimeric complex are

separated by a distance (74.3 Å) that, depending on linker flexibility, may be too great to accommodate contacts between associated 7TM domains (Fig. 5f). □

Methods

Protein expression and purification

We made a pFastBac Dual plasmid (Invitrogen) to encode both human FSH and human FSHR_{HB} under control of separate promoters for introduction into a baculovirus vector. The hormone construct comprises the signal peptide and entire mature sequence of FSH-β (residues 1–111) followed by a 15-residue linker (GGGSGGGSGGGSGGG) and the mature sequence of FSH-α (residues 1–92). The receptor construct comprises the native signal sequence followed by the FSHR_{HB} ectodomain (residues 1–268) and a Flag tag to facilitate purification. Hi5 cells infected with this recombinant baculovirus secreted the FSH–FSHR_{HB} complex, which we purified from the cell supernatant by affinity chromatography (anti-Flag antibody M2) and size exclusion chromatography (Superdex200). The yield of purified FSH–FSHR_{HB} was about 0.1 mg per litre of insect cell culture. We partially deglycosylated the complex using endoglycosidases F2 and F3, and purified the product by ion exchange chromatography (MonoQ).

Crystallization and data collection

Fully glycosylated FSH–FSHR_{HB} were crystallized from tert-butanol into large polyhedra. These crystals are in space group R32 (*a* = 227.2 Å, *α* = 80.3°) with an estimated five to ten complexes per asymmetric unit, but they diffract only to 9 Å spacings (NSLS beamline X4A). Partially deglycosylated FSH–FSHR_{HB} crystallized from PEG3350 and dilute Li₂SO₄ as clusters of thin plates (5–10 μm thick). These crystals belong to space group C2 (*a* = 121.3 Å, *b* = 66.9 Å, *c* = 148.6 Å and *β* = 99.1°) and have two FSH–FSHR_{HB} complexes per asymmetric unit. Diffraction extended to 2.9 Å spacings at APS beamline 31-ID of SGX-CAT, where we measured complete data that were reduced using Denzo and Scalepack⁴⁵ (Table 1).

Structure determination and refinement

We used molecular replacement and molecular averaging to solve the structure. A two-fold non-crystallographic symmetry (NCS) axis was identified from the self-rotation function, and the known structure of FSH⁷ was used as the search model in Amore⁴⁶ to locate both FSH molecules in the asymmetric unit. After rigid-body refinement against all data (2.5–2.9 Å), phases from this model were improved by two-fold NCS averaging in DM⁴⁷. The resulting electron-density map revealed a β-sheet in the receptor region as predicted for the LRR motif of FSHR_{HB}. We developed a complete atomic model of the complex through a succession of manual fittings and iterative averaging. Optimal NCS restraints were determined from an *R*_{free} analysis (Q.F. & W.A.H., unpublished data). We used O⁴⁸ for model building, CNS⁴⁹ for initial refinement and REFMAC⁴⁷ in the final stages. Refinement statistics are given in Table 1.

The final model contains two FSH molecules (residues α3–92 and α6'–92'; β3–107 and β3'–107'), two FSHR_{HB} molecules (residues 18–259 and 18'–250'), one mannose and ten *N*-acetylglucosamine residues, 50 water molecules, and three sulphate ions. Continuous density was observed for carbohydrate moieties at all *N*-linked glycosylation sites on one FSH–FSHR_{HB} complex (αN52, αN78, βN7 and βN24 of FSH; N191 of FSHR_{HB}) and three sites on the other (αN78' and βN24' of FSH'; N191' of FSHR_{HB}'). There was no density for residues of the Flag-tagged peptide and the FSH-β–FSH-α linker, presumably due to disordering. A Ramachandran analysis (http://kinemage.biochem.duke.edu) places 92.1% of all residues in favoured regions and 0.9% in outlier regions.

Chemical crosslinking

We carried out reactions of the FSH–FSHR_{HB} complex at concentrations up to 360 μM

Table 1 Diffraction data and refinement

Data collection	
Space group	C2
Bragg spacings (Å)	25–2.9 (3.0–2.9)
Total observations	85,886
Unique reflections	25,282 (2,494)
Completeness (%)	98.6 (97.7)
Average <i>I</i> / <i>σ</i> (<i>I</i>)	12.4 (3.4)
<i>R</i> _{sym} (%)*	6.9 (38.8)
Refinement (2.5–2.9 Å, <i> F </i> > 0)	
Reflections (work/test)	24,020/1,262
<i>R</i> _{work} (%)†	21.9 (29.7)
<i>R</i> _{free} (%)†	25.9 (35.6)
Average <i>B</i> -factors (Å ²)	56.3
r.m.s.d.	
Bonds (Å)	0.010
Angles (°)	1.427
<i>B</i> -factors (Å ²)	
Main-chain bonds/angles	1.95/2.88
Side-chain bonds/angles	2.90/4.23

Values in parentheses indicate the corresponding statistics in the highest-resolution shell. **R*_{sym} = (Σ|*I*_{*h*} – ⟨*I*_{*h*}⟩)/Σ*I*_{*h*}, where ⟨*I*_{*h*}⟩ is the average intensity over symmetry equivalent. †*R*_{work} = Σ||*F*_o – *F*_c||/Σ|*F*_o|. *R*_{free} is equivalent to *R*_{work}, but calculated for a randomly chosen 5% of reflections, which were omitted from the refinement process.

with fixed molar ratios of glutaraldehyde that were sufficiently low to prevent adventitious crosslinking at higher protein concentrations (30 lysines per complex). A concentration-dependent dimer band on native gels was quantified by densitometry. The dimer-band density (*D*) from this crosslinked subpopulation is proportional to the equilibrium dimer fraction, *D* = *Sy*, where *S* is a scaling factor, and the dimer fraction (*y*) depends on the total protein concentration (*C*_T) and *K*_d according to

$$y = \frac{(\sqrt{1 + 8C_T/K_d} - 1)}{(\sqrt{1 + 8C_T/K_d} + 1)}$$

A least-squares fitting of the *D*(*C*_T) data gave estimates of *S* and *K*_d.

Analytical ultracentrifugation

We carried out sedimentation equilibrium experiments using absorption optics in a Beckman XL-I analytical centrifuge. Purified fully glycosylated FSH–FSHR_{HB} was analysed at three concentrations (0.33, 0.66 and 1.05 mg ml⁻¹) and three rotor speeds (7,000, 9,000 and 12,000 r.p.m.). Data were analysed with WinNONLIN⁵⁰, floating the monomer mass to determine the extent of glycosylation. The FSH–FSHR_{HB} mass was found to be 78 kDa, implying 32% carbohydrate mass.

Dynamic light scattering

We measured hydrodynamic radii of FSH–FSHR_{HB} using a DynaPro molecular sizing instrument (Protein Solutions).

See supplementary information for details of the Methods.

Received 27 August; accepted 22 November 2004; doi:10.1038/nature03206.

- Dias, J. A. *et al.* Molecular, structural, and cellular biology of follitropin and follitropin receptor. *Vitam. Horm.* **64**, 249–322 (2002).
- Simoni, M., Gromoll, J. & Nieschlag, E. The follicle-stimulating hormone receptor: biochemistry, molecular biology, physiology, and pathophysiology. *Endocr. Rev.* **18**, 739–773 (1997).
- Themmen, A. P. N. & Huhtaniemi, I. T. Mutations of gonadotropins and gonadotropin receptors: elucidating the physiology and pathophysiology of pituitary-gonadal function. *Endocr. Rev.* **21**, 551–583 (2000).
- Pierce, J. G. & Parsons, T. F. Glycoprotein hormones: structure and function. *Annu. Rev. Biochem.* **50**, 465–495 (1981).
- Wu, H., Lustbader, J. W., Liu, Y., Canfield, R. E. & Hendrickson, W. A. Structure of human chorionic gonadotropin at 2.6 Å resolution from MAD analysis of the selenomethionyl protein. *Structure* **2**, 545–558 (1994).
- Laphorn, A. J. *et al.* Crystal structure of human chorionic gonadotropin. *Nature* **369**, 455–461 (1994).
- Fox, K. M., Dias, J. A. & Van Roey, P. Three-dimensional structure of human follicle-stimulating hormone. *Mol. Endocrinol.* **15**, 378–389 (2001).
- Ascoli, M., Fanelli, F. & Segaloff, D. L. The lutropin/choriogonadotropin receptor, a 2002 perspective. *Endocr. Rev.* **23**, 141–174 (2002).
- Szkudlinski, M. W., Fremont, V., Ronin, C. & Weintraub, B. D. Thyroid-stimulating hormone and thyroid-stimulating hormone receptor structure-function relationships. *Physiol. Rev.* **82**, 473–502 (2002).
- Hsu, S. Y. T. New insights into the evolution of the relaxin-LGR signaling system. *Trends Endocrinol. Metab.* **14**, 303–309 (2003).
- Sugahara, T. *et al.* Biosynthesis of a biologically active single peptide chain containing the human common α and chorionic gonadotropin β subunits in tandem. *Proc. Natl Acad. Sci. USA* **92**, 2041–2045 (1995).
- Narayan, P., Wu, C. & Puett, D. Functional expression of yoked human chorionic gonadotropin in baculovirus-infected insect cells. *Mol. Endocrinol.* **9**, 1720–1726 (1995).
- Schmidt, A., MacColl, R., Lindau-Shepard, B., Buckler, D. R. & Dias, J. A. Hormone-induced conformational change of the purified soluble hormone binding domain of follitropin receptor complexed with single chain follitropin. *J. Biol. Chem.* **276**, 23373–23381 (2001).
- Jiang, X. *et al.* Structural predictions for the ligand-binding region of glycoprotein hormone receptors and the nature of hormone-receptor interactions. *Structure* **3**, 1341–1353 (1995).
- Kobe, B. & Kajava, A. V. The leucine-rich repeat as a protein recognition motif. *Curr. Opin. Struct. Biol.* **11**, 725–732 (2001).
- Davis, D., Liu, X. & Segaloff, D. L. Identification of the sites of N-linked glycosylation on the follicle-stimulating hormone (FSH) receptor and assessment of their role in FSH receptor function. *Mol. Endocrinol.* **9**, 159–170 (1995).
- Bhowmick, N., Huang, J., Puett, D., Isaacs, N. W. & Laphorn, A. J. Determination of residues important in hormone binding to the extracellular domain of the luteinizing hormone/chorionic gonadotropin receptor by site-directed mutagenesis and modeling. *Mol. Endocrinol.* **10**, 1147–1159 (1996).
- Liu, C. & Dias, J. A. Long loop residues 33–58 in the human glycoprotein hormone common α subunit contain structural components for subunit heterodimerization and human follitropin-receptor binding. *Arch. Biochem. Biophys.* **329**, 127–135 (1996).
- Arnold, C. J. *et al.* The human follitropin α-subunit C terminus collaborates with a β-subunit cysteine noose and an α-subunit loop to assemble a receptor-binding domain competent for signal transduction. *Biochemistry* **37**, 1762–1768 (1998).
- Erickson, L. D. *et al.* Synthetic α-subunit peptides stimulate testosterone production *in vitro* by rat Leydig cells. *Endocrinology* **126**, 2555–2560 (1990).
- Leinung, M. C., Reed, D. K., McCormick, D. J., Ryan, R. J. & Morris, J. C. Further characterization of the receptor-binding region of the thyroid-stimulating hormone α subunit: a comprehensive synthetic peptide study of the α-subunit 26–46 sequence. *Proc. Natl Acad. Sci. USA* **88**, 9707–9711 (1991).
- Keutmann, H. T., Mason, K. A., Kitzmann, K. & Ryan, R. J. Role of the β 93–100 determinant loop sequence in receptor binding and biological activity of human luteinizing hormone and chorionic gonadotropin. *Mol. Endocrinol.* **3**, 526–531 (1989).
- Moyle, W. R. *et al.* Co-evolution of ligand-receptor pairs. *Nature* **368**, 251–255 (1994).

24. Dias, J. A., Zhang, Y. & Liu, X. Receptor binding and functional properties of chimeric human follitropin prepared by an exchange between a small hydrophilic intercysteine loop of human follitropin and human lutropin. *J. Biol. Chem.* **269**, 25289–25294 (1994).
25. Grossmann, M. *et al.* Substitution of the seat-belt region of the thyroid-stimulating hormone (TSH) β -subunit with the corresponding regions of choriogonadotropin or follitropin confers luteotropic but not follitropic activity to chimeric TSH. *J. Biol. Chem.* **272**, 15532–15540 (1997).
26. Smits, G. *et al.* Glycoprotein hormone receptors: determinants in leucine-rich repeats responsible for ligand specificity. *EMBO J.* **22**, 2692–2703 (2003).
27. Vischer, H. F., Granneman, J. C. M. & Bogerd, J. Opposite contribution of two ligand-selective determinants in the N-terminal hormone-binding exodomain of human gonadotropin receptors. *Mol. Endocrinol.* **17**, 1972–1981 (2003).
28. Chen, F., Wang, Y. & Puett, D. The carboxy-terminal region of the glycoprotein hormone α -subunit: contributions to receptor binding and signaling in human chorionic gonadotropin. *Mol. Endocrinol.* **6**, 914–919 (1992).
29. Strader, C. D., Fong, T. M., Tota, M. R., Underwood, D. & Dixon, R. A. Structures and function of G protein-coupled receptors. *Annu. Rev. Biochem.* **63**, 101–132 (1994).
30. Palczewski, K. *et al.* Crystal structure of rhodopsin: a G protein-coupled receptor. *Nature* **289**, 739–745 (2000).
31. Remy, J. *et al.* Mapping of HCG-receptor complexes. *Mol. Cell. Endocrinol.* **125**, 79–91 (1996).
32. Braun, T., Schofield, P. R. & Sprengel, R. Amino-terminal leucine-rich repeats in gonadotropin receptors determine hormone selectivity. *EMBO J.* **10**, 1885–1890 (1991).
33. Vassart, G., Pardo, L. & Costagliola, S. A molecular dissection of the glycoprotein hormone receptors. *Trends Biochem. Sci.* **29**, 119–120 (2004).
34. Kunishima, N. *et al.* Structural basis of glutamate recognition by a dimeric metabotropic glutamate receptor. *Nature* **407**, 971–977 (2000).
35. Costagliola, S. *et al.* Tyrosine sulfation is required for agonist recognition by glycoprotein hormone receptors. *EMBO J.* **21**, 504–513 (2002).
36. Szkudlinski, M. W., Teh, N. G., Grossmann, M., Tropea, J. E. & Weintraub, B. D. Engineering human glycoprotein hormone superactive analogues. *Nature Biotechnol.* **14**, 1257–1263 (1996).
37. Heikoop, J. C. *et al.* Partially deglycosylated human choriogonadotropin, stabilized by intersubunit disulfide bonds, shows full bioactivity. *Eur. J. Biochem.* **253**, 354–356 (1998).
38. Ji, I., Zeng, H. & Ji, T. H. Receptor activation and signal generation by the lutropin/choriogonadotropin receptor. *J. Biol. Chem.* **268**, 22971–22974 (1993).
39. Terrillon, S. & Bouvier, M. Roles of G-protein-coupled receptor dimerization. From ontogeny to signaling regulation. *EMBO Rep.* **5**, 30–34 (2004).
40. Grasberger, B., Minton, A. P., DeLisi, C. & Metzger, H. Interactions between proteins localized in membranes. *Proc. Natl Acad. Sci. USA* **83**, 6258–6262 (1986).
41. Osuga, Y. *et al.* Co-expression of defective luteinizing hormone receptor fragments partially reconstitutes ligand-induced signal generation. *J. Biol. Chem.* **272**, 25006–25012 (1997).
42. Ji, I. *et al.* Trans-activation of mutant follicle-stimulating hormone receptors selectively generates only one of two hormone signals. *Mol. Endocrinol.* **18**, 968–978 (2004).
43. Tao, Y. X., Johnson, N. B. & Segaloff, D. L. Constitutive and agonist-dependent self-association of the cell surface human lutropin receptor. *J. Biol. Chem.* **279**, 5904–5914 (2004).
44. Roess, D. A. & Smith, S. M. L. Self-association and raft localization of functional luteinizing hormone receptors. *Biol. Reprod.* **69**, 1765–1770 (2003).
45. Otwinowski, Z. & Minor, W. Processing of X-ray diffraction data collected in oscillation mode. *Methods Enzymol.* **276**, 307–326 (1997).
46. Navaza, J. Implementation of molecular replacement in AMoRe. *Acta Crystallogr. D* **57**, 1367–1372 (2001).
47. Collaborative Computational Project, Number 4. The CCP4 suite: Programs for protein crystallography. *Acta Crystallogr. D* **50**, 760–776 (1994).
48. Jones, T. A., Zou, J. Y., Cowan, S. W. & Kjeldgaard, M. Improved methods for building protein models in electron density maps and the location of errors in the models. *Acta Crystallogr. A* **47**, 110–119 (1991).
49. Brünger, A. T. *et al.* Crystallography & NMR system: A new software suite for macromolecular structure determination. *Acta Crystallogr. D* **54**, 905–921 (1998).
50. Laue, T. M., Shah, B. D., Ridgeway, T. M. & Pelletier, S. L. in *Analytical Ultracentrifugation in Biochemistry and Polymer Science* (eds Harding, S. E., Rowe, A. J. & Horton, J. C.) 90–125 (Royal Society of Chemistry, Cambridge, 1992).

Supplementary Information accompanies the paper on www.nature.com/nature.

Acknowledgements We thank J. Lustbader and L. Lobel for discussion and access to the cDNA clones of human FSHR and FSH, which were originally provided by A. Hsueh and W. Moyle; N. Belgado and D. Hildesheim for help with insect cell culture work; T. Laue, R. Olson and E. Gouaux for advice on analytical ultracentrifugation experiments; M. A. Gawinowicz for sequencing and mass spectrometry; R. Henderson and R. Kovall for critical reading of the manuscript; L. Mosyak, J. Cheung, G. Gregorio, V. Grantcharova, D. Garboczi, C. Lusty and R. Jin for discussion; and synchrotron beamline staff for assistance with data collection. Beamline X4A at the National Synchrotron Light Source (NSLS) is supported by the New York Structural Biology Center, and beamline 31-ID at the Advanced Photon Source (APS) is supported by Structural GenomiX, Inc. NSLS and APS are Department of Energy facilities. Work was supported in part by a NIH grant. Q.R.F. is an Agouron Institute fellow of the Jane Coffin Childs Memorial Foundation.

Competing interests statement The authors declare that they have no competing financial interests.

Correspondence and requests for materials should be addressed to W.A.H. (wayne@convex.hhmi.columbia.edu). Atomic coordinates and structure factors have been deposited into the Protein Data Bank under accession code 1XWD.